

# Molecular beam epitaxy of boron doped p-type BaSi<sub>2</sub> epitaxial films on Si(111) substrates for thin-film solar cells

著者別名	都甲 薫, 末益 崇
journal or publication title	Journal of crystal growth
volume	378
page range	201-204
year	2013-09
権利	(C) 2013 Elsevier B.V. NOTICE: this is the author's version of a work that was accepted for publication in Journal of crystal growth. Changes resulting from the publishing process, such as peer review, editing, corrections, structural formatting, and other quality control mechanisms may not be reflected in this document. Changes may have been made to this work since it was submitted for publication. A definitive version was subsequently published in Journal of crystal growth, 378, 2013 <a href="http://dx.doi.org/10.1016/j.jcrysgr.2012.12.153">http://dx.doi.org/10.1016/j.jcrysgr.2012.12.153</a>
URL	<a href="http://hdl.handle.net/2241/119793">http://hdl.handle.net/2241/119793</a>

doi: 10.1016/j.jcrysgr.2012.12.153

1 **Molecular beam epitaxy of boron doped  $p$ -type BaSi<sub>2</sub> epitaxial films on**  
2 **Si(111) substrates for thin-film solar cells**

3

4 M. Ajmal Khan,<sup>a</sup> Kosuke O. Hara,<sup>b</sup> Kotaro Nakamura,<sup>a</sup> Weijie Du,<sup>a</sup> Masakazu Baba,<sup>a</sup>  
5 Katsuaki Toh,<sup>a</sup> Mitsushi Suzuno,<sup>a</sup> Kaoru Toko,<sup>a</sup> Noritaka Usami,<sup>b,c</sup> and  
6 Takashi Suemasu<sup>a,c</sup>

7

8 <sup>a</sup>*Institute of Applied Physics, University of Tsukuba, Tsukuba, Ibaraki 305-8573, Japan*

9 <sup>b</sup>*Institute for Materials Research, Tohoku University, Sendai, Miyagi 980-8577, Japan*

10 <sup>c</sup>*Japan Science and Technology Agency, CREST, Chiyoda, Tokyo 102-0075, Japan*

11

12 **Corresponding author:** Prof. T. Suemasu

13 Institute of Applied Physics, University of Tsukuba, Tsukuba, Ibaraki 305-8573, Japan

14 TEL/FAX: +81-29-853-5111, Email: suemasu@bk.tsukuba.ac.jp

15

16

17 **Abstract**

18 We have successfully grown *a*-axis-oriented *p*-type BaSi<sub>2</sub> films on Si(111) by *in situ* boron  
19 (B) doping using molecular beam epitaxy (MBE). The hole concentration in B-doped BaSi<sub>2</sub>  
20 was controlled in the range between 10<sup>17</sup> and 10<sup>19</sup> cm<sup>-3</sup> at room temperature by changing the  
21 temperature of the B Knudsen cell crucible. The acceptor level was estimated to be  
22 approximately 23 meV.

23

24

25 PACS: 78.40.Fy

26

27 **Keywords:** B1. semiconducting silicides; B2. BaSi<sub>2</sub>; B3. solar cell; A3. MBE; A1. impurity  
28 doping

29

## 30 **1. Introduction**

31 It is important for solar cell materials to have a large absorption coefficient and a  
32 suitable band gap to yield high conversion efficiency. Materials that are composed of  
33 abundant and non-toxic elements are also desirable. Among such materials we have focused  
34 on semiconducting BaSi<sub>2</sub>. The BaSi<sub>2</sub> has the orthorhombic lattice (space group Pnma) with a  
35 unit cell containing 8 Ba and 16 Si atoms, the latter of which form Si<sub>4</sub> tetrahedra and can thus  
36 be considered as Zintl phase [1,2]. Semiconducting BaSi<sub>2</sub> has the indirect band gap of  
37 approximately 1.3 eV matching the solar spectrum and has a very large absorption coefficient  
38 of  $3 \times 10^4 \text{ cm}^{-1}$  at 1.5 eV [3-5]. Optical absorption measurements have shown that the band gap  
39 of BaSi<sub>2</sub> can be increased up to 1.4 eV by replacing half of the Ba atoms in BaSi<sub>2</sub> with  
40 isoelectric Sr atoms [6], which is in agreement with the theoretical calculations [7-9].  
41 Recently, we successfully achieved large photoresponsivity and internal quantum efficiency  
42 exceeding 70% in *a*-axis-oriented BaSi<sub>2</sub> epitaxial layers grown by molecular beam epitaxy  
43 (MBE) [10-13]. These results have spurred interest in this material. The basic structure of a  
44 solar cell is a *p-n* junction. Therefore, control of the conductivity of BaSi<sub>2</sub> by impurity doping  
45 is a requirement. The carrier concentration of undoped *n*-BaSi<sub>2</sub> is approximately  $5 \times 10^{15} \text{ cm}^{-3}$   
46 [4]. According to Imai and Watanabe [14,15], substitution of Si in the BaSi<sub>2</sub> lattice is more  
47 favorable than substitution of Ba from an energetic point of view by first-principles  
48 calculation. In our previous works, the electron concentration of Sb-doped BaSi<sub>2</sub> was

49 controlled in the range between  $10^{16}$  and  $10^{20}$   $\text{cm}^{-3}$  at room temperature (RT). In contrast, Al-  
50 and In-doped  $\text{BaSi}_2$  show  $p$ -type conductivity, but the hole concentration was limited up to  
51  $3 \times 10^{17}$   $\text{cm}^{-3}$  [16-19]. Thus, it is highly required to find another impurity atom for heavily  
52  $p$ -type doping of  $\text{BaSi}_2$ . In this article, we chose to adopt boron (B) as an alternative impurity  
53 and aimed to achieve  $p$ -type doping of over  $10^{19}$   $\text{cm}^{-3}$  in  $\text{BaSi}_2$  films by MBE.

54

## 55 **2. Experimental**

56 Details of the growth procedure for *in situ* impurity doped  $\text{BaSi}_2$  films have been previously  
57 described for In- and Sb-doped  $\text{BaSi}_2$  [17]. An ion-pumped MBE system equipped with  
58 standard Knudsen cells (K-cells) for Ba and B, and an electron-beam evaporation source for  
59 Si was used. For electrical measurements, high-resistivity floating-zone (FZ)  $n$ -Si(111) ( $\rho >$   
60  $1000 \text{ } \Omega\cdot\text{cm}$ ) substrates were used. Briefly, MBE growth of B-doped  $\text{BaSi}_2$  films was carried  
61 out as follows. Firstly, a 10-nm-thick  $\text{BaSi}_2$  epitaxial film was grown on Si(111) at  $600 \text{ } ^\circ\text{C}$  by  
62 reactive deposition epitaxy (RDE; Ba deposition on a hot Si substrate), and this was used as a  
63 template for the  $\text{BaSi}_2$  overlayers. Next, Ba, Si, and B were co-evaporated at  $600 \text{ } ^\circ\text{C}$  onto the  
64  $\text{BaSi}_2$  template to form impurity-doped  $\text{BaSi}_2$  by MBE. The thickness of the grown layers  
65 including the template was approximately 200-250 nm. The temperature of B,  $T_B$ , was varied  
66 from 1250 to 1575  $^\circ\text{C}$  in samples A-G. The deposition rates of Si and Ba were approximately  
67 1.5 and 4.0 nm/min, respectively. Sample preparation was summarized in Table 1. It turned

68 out that it was difficult to make ohmic contacts with Au/Cr on as-grown B-doped BaSi<sub>2</sub> films  
69 for samples grown at  $T_B \leq 1500^\circ\text{C}$ . Thus rapid thermal annealing (RTA) was performed at  
70 800 °C for 30 s in an Ar atmosphere with heating rate of 40°C/s for (samples C-G) prior to the  
71 deposition of Au/Cr electrodes.

72 The crystal quality of the already grown layers was characterized by X-ray diffraction  
73 (XRD) and reflection high-energy electron diffraction (RHEED) measurements. The electrical  
74 properties were characterized by Hall measurements using the van der Pauw method. The  
75 applied magnetic field was 0.5–0.7 T, normal to the sample surface. Secondary ion mass  
76 spectroscopy (SIMS) measurements using O ions were performed to investigate the depth  
77 profile of B doped. Reference samples with a controlled number of B atoms doped in BaSi<sub>2</sub>  
78 have not yet been prepared but will be necessary to precisely determine the impurity  
79 concentration by SIMS.

80

### 81 **3. Results and discussion**

82 Figure 1 shows the  $\theta$ -2 $\theta$  XRD patterns of B-doped as-grown BaSi<sub>2</sub> films with  
83  $T_B = 1250$ - $1575^\circ\text{C}$ . The diffraction peaks of (100)-oriented BaSi<sub>2</sub>, such as (200), (400) and  
84 (600), are dominant in the  $\theta$ -2 $\theta$  XRD patterns. These peaks match the epitaxial relationship  
85 between BaSi<sub>2</sub> and Si. The forbidden diffraction peak designated by (\*) is considered to be  
86 due to double diffraction. Further increase of  $T_B$  resulted in two new diffraction peaks of

87 rhombohedral B(110) around  $2\theta=36^\circ$  and B(220) at  $2\theta=77^\circ$ . This means that the crystalline  
88 quality starts to deteriorate with increasing the amount of B atoms in the BaSi<sub>2</sub> films. Figures  
89 2(a)-2(h) present the streaky RHEED patterns of B-doped as-grown BaSi<sub>2</sub> films prepared with  
90  $T_B=1250-1575^\circ\text{C}$ , respectively, observed along the Si[11-2] azimuth, indicating that the  
91 BaSi<sub>2</sub> films were grown successfully. Figs. 3(a) and 3(b) show the SIMS depth profiles of B  
92 concentration  $N_B$  in the B-doped as-grown BaSi<sub>2</sub> films prepared with  $T_B=1450$  and  $1550^\circ\text{C}$ ,  
93 respectively. The doped B atoms are uniformly distributed in the grown layers in both samples,  
94 and they did not show any diffusion tendency. Similar results were also obtained in other  
95 samples. The averaged value of  $N_B$  for BaSi<sub>2</sub> prepared with  $T_B=1450^\circ\text{C}$  is approximately  
96  $2\times 10^{21}\text{ cm}^{-3}$  in Fig. 3(a), while that with  $T_B=1550^\circ\text{C}$  is  $1\times 10^{22}\text{ cm}^{-3}$  in Fig. 3(b). This result is  
97 explained relatively well by the difference in vapor pressure of B; The vapor pressure of B at  
98  $1550^\circ\text{C}$  is approximately 7 times larger than that at  $1450^\circ\text{C}$  [20]. These results mean that the  
99 concentration of B atoms in the BaSi<sub>2</sub> can be controlled by  $T_B$ . The B concentrations in the  
100 SIMS profiles shown in Fig. 3 were corrected using reference samples, where controlled  
101 number of B atoms was doped in the BaSi<sub>2</sub> films by ion implantations. The activation rate of  
102 B atoms can be thus estimated, that is approximately  $p=10^{19}\text{ cm}^{-3}/N_B=10^{22}\text{ cm}^{-3}\cong 0.1\%$  for  
103 sample H. But it was found from plan-view transmission electron microscopy images and also  
104 from the  $\theta$ - $2\theta$  XRD patterns that some amounts of B atoms were in the form of B clusters.  
105 Thus the actual B activation rate in the BaSi<sub>2</sub> film is supposed to be much higher than the

106 above value of 0.1%, and it is approximately 1% for sample H. The reason of such a small  
107 activation rate of B is probably attributed to relatively low growth temperature of 600°C and  
108 too much B concentrations.

109 We next move on to the electrical properties of B-doped as-grown BaSi<sub>2</sub> films,  
110 samples H and I. The hole concentration  $p$  was  $1.0 \times 10^{19}$  for sample H, and  $2.5 \times 10^{18} \text{ cm}^{-3}$  for  
111 sample I at RT. These values are the highest ever reported for  $p$ -type BaSi<sub>2</sub>. We speculate that  
112 defects induced by crystallized B in the BaSi<sub>2</sub> film could cause the reduced  $p$  in sample I. In  
113 order to evaluate the acceptor level  $E_A$  in sample H, we performed the temperature  
114 dependence of  $p$ . To secure the ohmic contacts on the surface at lower temperatures, first the  
115 temperature dependence of current-voltage ( $I$ - $V$ ) characteristics were measured as shown in  
116 Fig. 4(a). Ohmic behavior was confirmed over the wide temperature range between 30 and  
117 300 K. Resistance increases with decreasing temperature in Fig. 4(a), which is typical for  
118 semiconductors. Fig. 4(b) gives the temperature dependence of  $p$  for sample H. The acceptor  
119 level calculated using Eq. (1) was about 23 meV.

$$120 \quad p \propto \exp\left(-\frac{E_A}{2k_B T}\right) \quad (1)$$

121 Here,  $k_B$  is the Boltzmann's constant, and  $T$  the absolute temperature. This  $E_A$  value is much  
122 smaller than that in Al-doped BaSi<sub>2</sub> ( $E_A=50$ , and 140 meV) [18]. Such a shallow  $E_A$  level of  
123 23 meV could be the reason for heavily  $p$ -type doping in sample H. Regarding the other  
124 samples, it was difficult to obtain reliable hole concentration and mobility data at RT. Thus,



125 we performed the RTA treatment on samples C-I to achieve activation of doped B atoms. The  
126 obtained  $p$  and hole mobility  $\mu_h$  were summarized in Table 1. The hole concentration  
127 increases gradually from  $10^{17}$  to  $10^{19}$   $\text{cm}^{-3}$  with increasing  $T_B$ , thereby showing that the RTA is  
128 a very effective means to activate the B atoms.

129 Figure 5 shows the measured  $\mu_h$  versus  $p$  for B-doped  $\text{BaSi}_2$ . As the hole  
130 concentration increases the mobility decreases. This trend is usually predicted by ionized  
131 impurity scattering in conventional semiconductors. The hole mobilities are always smaller  
132 than the electron mobilities in Sb-doped  $\text{BaSi}_2$  [17]. According to Migas *et al.*, this is  
133 attributed to a larger effective mass for holes than electrons [3]. The  $p$  value reached a  
134 maximum of  $3.4 \times 10^{19}$   $\text{cm}^{-3}$ , and the resistivity was  $0.02 \Omega \cdot \text{cm}$  in sample G. At present, only  
135 limited information has been obtained for the electrical properties of B-doped  $\text{BaSi}_2$ . We  
136 speculate that both growth temperatures during MBE and RTA duration influence the  
137 electrical properties of B-doped  $\text{BaSi}_2$ . Thus, further studies are necessary in order to optimize  
138 the growth condition for B-doped  $\text{BaSi}_2$  films by MBE.

139

#### 140 **4. Conclusions**

141 We achieved the hole concentration of over  $10^{19}$   $\text{cm}^{-3}$  at RT in *in situ* B-doped  $\text{BaSi}_2$   
142 films by MBE. The acceptor level was estimated to be approximately 23 meV from the  
143 temperature dependence of hole concentration. The RTA treatment performed at 800 °C for

144 30 s in Ar activated the B atoms in the BaSi<sub>2</sub> films. The hole concentration increased by the  
145 RTA treatment and reached a maximum of  $3.4 \times 10^{19} \text{ cm}^{-3}$  for BaSi<sub>2</sub> prepared with  
146  $T_B=1550 \text{ }^\circ\text{C}$ .

147

#### 148 **Acknowledgements**

149           The authors would like to thanks Prof. Tanimoto of the University of Tsukuba for his  
150 kind help for XRD measurements, Dr. Imai of AIST for useful discussion. We would also like  
151 to thank Dr. Mitsushi Suzuno for the helpful discussions and valuable comments during the  
152 course of this research. This work was supported in part by Core Research for Evolutional  
153 Science and Technology (CREST) of the Japan Science and Technology Agency.

154

155 **References**

- 156 [1] J. Evers, G. Oehlinger, A. Weiss, *Angew. Chem., Int. Ed.*, 16 (1977) 659.
- 157 [2] M. Imai, T. Hirano, *J. Alloys Compd.* 224 (1995) 111.
- 158 [3] D.B. Migas, V.L. Shaposhnikov, V.E. Borisenko, *Phys. Status Solidi B* 244 (2007) 2611.
- 159 [4] K. Morita, Y. Inomata, T. Suemasu, *Thin Solid Films* 508 (2006) 363.
- 160 [5] K. Toh, T. Saito, T. Suemasu, *Jpn. J. Appl. Phys.* 50 (2011) 068001.
- 161 [6] K. Morita, Y. Inomata, T. Suemasu, *Jpn. J. Appl. Phys.* 45 (2006) L390.
- 162 [7] Y. Imai, A. Watanabe, *Thin Solid Films* 515 (2007) 8219.
- 163 [8] Y. Imai, A. Watanabe, *Intermetallics* 18 (2010) 348.
- 164 [9] Y. Imai, A. Watanabe, *Intermetallics* 18 (2010) 1432.
- 165 [10] W. Du, M. Suzuno, M. A Khan, K. Toh, M. Baba, K. Nakamura, K. Toko, N. Usami, T.  
166 Suemasu, *Appl. Phys. Lett.* 100 (2012) 152114.
- 167 [11] Y. Matsumoto, D. Tsukada, R. Sasaki, M. Takeishi, T. Suemasu, *Appl. Phys. Express* 2  
168 (2009) 021101.
- 169 [12] D. Tsukada, Y. Matsumoto, R. Sasaki, M. Takeishi, T. Saito, N. Usami, T. Suemasu, *Appl.*  
170 *Phys. Express* 2 (2009) 051601.
- 171 [13] T. Saito, Y. Matsumoto, M. Suzuno, M. Takeishi, R. Sasaki, N. Usami, T. Suemasu,  
172 *Appl. Phys. Express* 3 (2009) 021301.
- 173 [14] Y. Imai, A. Watanabe, *Intermetallics* 15 (2007) 1291.

- 174 [15] Y. Imai, A. Watanabe, *Intermetallics* 19 (2011) 1102.
- 175 [16] M. Kobayashi, K. Morita, T. Suemasu, *Thin Solid Films* 515 (2007) 8242.
- 176 [17] M. Kobayashi, Y. Matsumoto, Y. Ichikawa, D. Tsukada, T. Suemasu, *Appl. Physics*  
177 *Express* 1 (2008) 051403.
- 178 [18] M. Takeishi, Y. Matsumoto, R. Sasaki, T. Saito, T. Suemasu, *Physics Procedia* 11 (2011)  
179 27.
- 180 [19] M. Ajmal Khan, M. Takeishi, Y. Matsumoto, T. Saito, and T. Suemasu, *Physics Procedia*  
181 11 (2011) 11.
- 182 [20] D. Stull, *American Institute of Physics Handbook, Third Edition*, McGraw Hill, New  
183 York, 1972.
- 184
- 185

186 **Figure Captions**

187

188 Fig. 1  $\theta$ - $2\theta$  XRD patterns of B-doped BaSi<sub>2</sub> films grown at  $T_B=1250$ - $1575$  °C.

189

190 Fig. 2 RHEED patterns of B-doped BaSi<sub>2</sub> films when  $T_B$  is (a) 1250, (b) 1300, (c) 1350, (d)  
191 1400, (e) 1450, (f) 1500, (g) 1550, and (h) 1575 °C, observed along the Si[11-2] azimuth.

192

193 Fig. 3. SIMS profiles of B for BaSi<sub>2</sub> films grown at  $T_B=(a)$  1450 and (b) 1550 °C.

194

195 Fig. 4. Temperature dependence of (a)  $I$ - $V$  characteristics and (b)  $p$  for B-doped as-grown  
196 BaSi<sub>2</sub> films grown with  $T_B=1550$  °C (sample G).

197

198 Fig. 5. Relationship of measured  $\mu_h$  versus  $p$  for B-doped BaSi<sub>2</sub> films at RT.

199

200

201

202

203

204 Table 1 Sample preparation: B temperature, annealing temperature and duration during RTA,  
 205 measured hole concentration and mobility are shown.

206

207	Sample	$T_B$	RTA	$p$	$\mu_p$
208		(°C)		(cm <sup>-3</sup> )	(cm <sup>2</sup> /V·s)
209	A	1250	w/o	-	-
210					
211	B	1300	w/o	-	-
212					
213	C	1350	800 °C /30 s	$8.5 \times 10^{16}$	23
214					
215	D	1400	800 °C /30 s	$1.2 \times 10^{17}$	168
216					
217	E	1450	800 °C /30 s	$5.0 \times 10^{17}$	59
218					
219	F	1500	800 °C /30 s	$5.2 \times 10^{17}$	17
220					
221	G	1550	800 °C /30 s	$3.4 \times 10^{19}$	8.3
222					
223	H	1550	w/o	$1.0 \times 10^{19}$	6.3
224					
225	I	1575	w/o	$2.5 \times 10^{18}$	8.3
226					

227

228

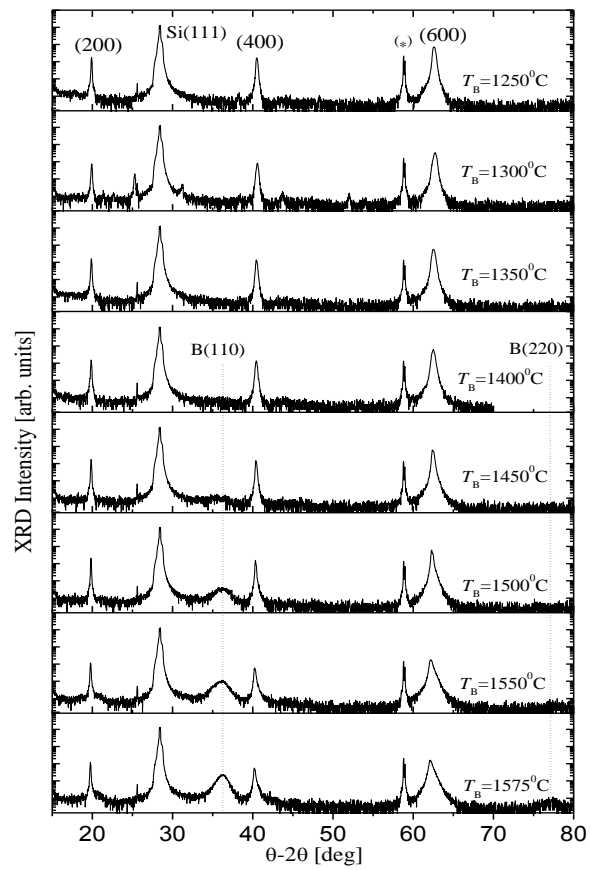


Fig. 1

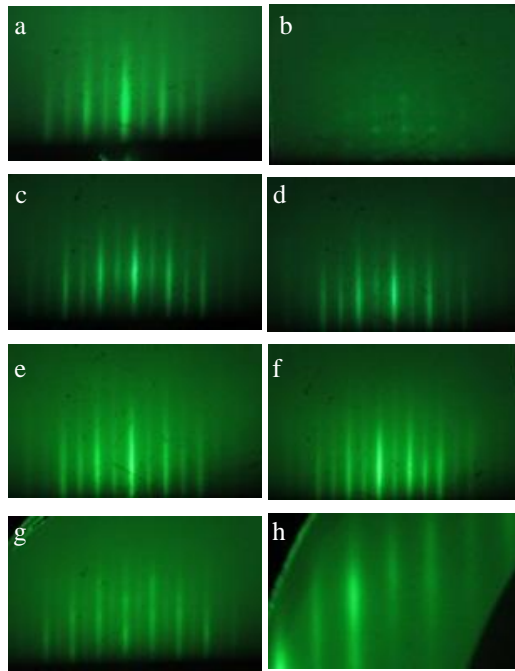


Fig. 2



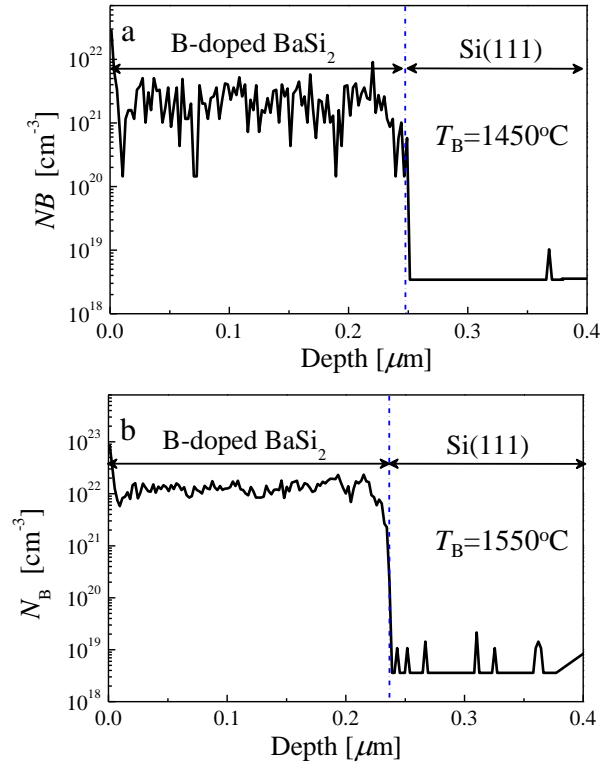


Fig. 3

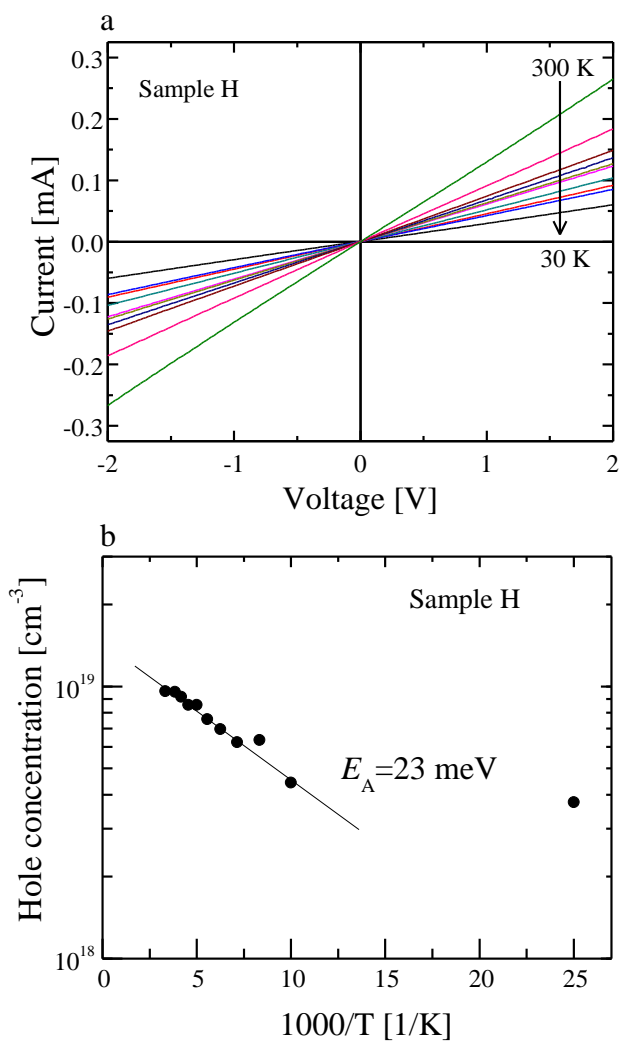


Fig. 4

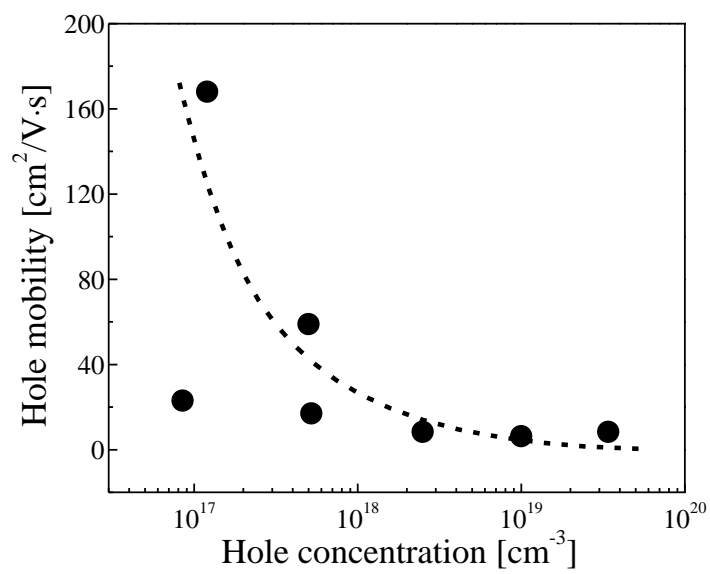


Fig. 5